



HAL
open science

Aggregates Associated with Instability of Antibodies during Aerosolization Induce Adverse Immunological Effects

Thomas Sécher, Elsa Bodier-Montagutelli, Christelle Parent, Laura Bouvart, Mélanie Cortes, Marion Ferreira, Ronan Macloughlin, Guy Ilango, Otmar Schmid, Renaud Respaud, et al.

► **To cite this version:**

Thomas Sécher, Elsa Bodier-Montagutelli, Christelle Parent, Laura Bouvart, Mélanie Cortes, et al.. Aggregates Associated with Instability of Antibodies during Aerosolization Induce Adverse Immunological Effects. *Pharmaceutics*, 2022, 14 (3), pp.671. 10.3390/pharmaceutics14030671 . hal-03687448

HAL Id: hal-03687448

<https://univ-tours.hal.science/hal-03687448>

Submitted on 3 Jun 2022

HAL is a multi-disciplinary open access archive for the deposit and dissemination of scientific research documents, whether they are published or not. The documents may come from teaching and research institutions in France or abroad, or from public or private research centers.

L'archive ouverte pluridisciplinaire **HAL**, est destinée au dépôt et à la diffusion de documents scientifiques de niveau recherche, publiés ou non, émanant des établissements d'enseignement et de recherche français ou étrangers, des laboratoires publics ou privés.

1 Article

2 **Aggregates associated with instability of antibodies during**
3 **aerosolization induce adverse immunological effects**4 **Thomas Secher**^{1,2}, **Elsa Bodier-Montagutelli**^{1,2,3#}, **Christelle Parent**^{1,2,#}, **Laura Bouvart**^{1,2,4}, **Mélanie Cortes**^{1,2}, **Marion**
5 **Ferreira**^{1,2,5}, **Guy Ilango**^{1,2}, **Otmar Schmid**⁶, **Renaud Respaud**^{1,2,3} and **Nathalie Heuzé-Vourc'h**^{1,2,*}6 ¹. INSERM, Centre d'Etude des Pathologies Respiratoires, U1100, F-37032 Tours, France.7 ². Université de Tours, F-37032 Tours, France.8 ³. CHRU de Tours, Service de Pharmacie, F-37032 Tours, France9 ⁴. CHRU de Tours, Département de Médecine pédiatrique, F-37032 Tours, France.10 ⁵. CHRU de Tours, Département de Pneumologie et d'exploration respiratoire fonctionnelle, F-37032 Tours,
11 France12 ⁶. Institute of Lung Health and Immunology and Comprehensive Pneumology Center with the CPC-M bioAr-
13 chive, Helmholtz Zentrum München, Member of the German Center for Lung Research (DZL), 85764 Neu-
14 herberg/Munich, Germany

15 * Correspondence: nathalie.vourch@med.univ-tours.fr;

16 **Abstract:**17 Background: Immunogenicity refers to the inherent ability of a molecule to stimulate an immune
18 response. Aggregates are one of the major risk factors for undesired immunogenicity of therapeutic
19 antibodies (Ab) and may ultimately result in immune-mediated adverse effects. For Ab delivered
20 by inhalation, it is necessary to consider the interaction between aggregates resulting from the in-
21 stability of the Ab during aerosolization and the lung mucosa. The aim of this study was to deter-
22 mine the impact of aggregates produced during aerosolization of therapeutic Ab on the immune
23 system.24 Methods: Human and murine immunoglobulin G (IgG) were aerosolized using a clinical-
25 ly-relevant nebulizer and their immunogenic potency was assessed both *in vitro* using a standard
26 human monocyte-derived dendritic cell (MoDC) reporter assay and *in vivo* in immune cells in the
27 airway compartment, lung parenchyma and spleen of healthy C57BL/6 mice after pulmonary
28 administration.Citation: Lastname, F.; Lastname, F.;
Lastname, F. Title. *Pharmaceutics*
2022, 14, x.
<https://doi.org/10.3390/xxxxx>Academic Editor: Firstname
Lastname

Received: date

Accepted: date

Published: date

Publisher's Note: MDPI stays
neutral with regard to jurisdictional
claims in published maps and
institutional affiliations.**Copyright:** © 2022 by the authors.Submitted for possible open access
publication under the terms and
conditions of the Creative CommonsAttribution (CC BY) license
(<https://creativecommons.org/licenses/by/4.0/>).29 Results: IgG aggregates, produced during nebulization, induced a dose-dependent activation of
30 MoDC characterized by enhanced production of cytokines and expression of co-stimulatory
31 markers. Interestingly, *in vivo* administration of high amounts of nebulization-mediated IgG ag-
32 gregates resulted in a profound and sustained local and systemic depletion of immune cells, which
33 was attributable to cell death. This cytotoxic effect was observed when nebulized IgG was admin-
34 istered locally in the airways as compared to a systemic administration but was mitigated by im-
35 proving IgG stability during nebulization, through the addition of polysorbates to the formulation.36 Conclusion: Although inhalation delivery represents an attractive alternative route for delivering
37 Ab to treat respiratory infections, our findings indicate that it is critical to prevent IgG aggregation
38 during the nebulization process to avoid pro-inflammatory and cytotoxic effects. Optimization of
39 Ab formulation can mitigate adverse effects induced by nebulization.**Keywords:** therapeutic antibody, aerosol, aggregates, immunogenicity

1. Introduction

Therapeutic antibodies (Ab), which mainly consist of monoclonal IgG, represent the fastest growing class of protein therapeutics, accounting for 90% of proteins on the market [1]. As recently highlighted during the COVID-19 pandemic, Ab have a tremendous potential to provide a rapid neutralizing response to emerging viral respiratory pathogens, augmenting vaccines for control of respiratory infections. Interestingly, both pulmonary and nasal delivery of therapeutic proteins are receiving increasing interest, as the airways are a relevant non-invasive entry portal to the respiratory tract for local-acting protein therapeutics [2-4]. For the treatment of respiratory diseases, several preclinical studies demonstrated that inhaled protein therapeutics, including Ab, are efficacious and display a better pharmacokinetic profile, as compared to other routes [5-7]. Despite recent clinical development of oral anti-infective Ab, in the context of the global response to SARS-CoV2 pandemic, the inhalation route remains unexploited for Ab. One of the unknowns is the biological consequence of Ab instability during aerosolization. Inhalation requires transformation of a (bulk) protein formulation in an aerosol, i.e., dispersion of a solution/suspension or a dry-powder dispersed into micron-sized particles suspended in a gaseous medium. As with 75% of the inhaled protein therapeutics in clinical development, nebulization of liquid formulations is often the primary technique used for inhalation of proteins [5]. Nebulization generates a huge air-liquid interface which, combined with the potential for nebulization-induced temperature increase and/or shear forces, can be deleterious for proteins. In response to such stresses, proteins are prone to unfolding, aggregating and, in some cases, being partly inactivated [8,9]. Aggregation is a key marker of instability of full-length Ab during nebulization [10,11] and its extent mainly depends on the type of Ab, the aerosol generator type and the formulation characteristics.

Aggregates are associated with Ab-related adverse immunogenicity [12-14]. Immunogenicity refers to the inherent properties of a molecule to stimulate an immune response. Adverse immunogenicity is due to uncontrolled and protracted immune responses and has major consequences on product safety and pharmacology [15-17]. For instance, adverse immunogenicity is associated with patient's immunization and production of anti-drug antibodies (ADAs) and affects protein therapeutics pharmacokinetics (PK), pharmacodynamics, efficacy, and safety, sometimes resulting in extremely harmful side effects [18,19]. To date, many factors have been implicated in adverse immunogenicity [20-23] and they include the content of aggregates and the route of administration, which are important parameters of Ab inhalation.

After inhalation, aggregates from aerosolized Ab will encounter the airways immune system, which has evolved over time to recognize, and prevent foreign particles, including aggregates, from penetrating the body. The airway mucosa is sentinelled by a high density of antigen-presenting cells (APC) that quickly and efficiently orchestrate local immune responses against inhaled antigens [24]. In the present study, we analyzed, both *in vitro* and *in vivo*, the immunological consequences of Ab aggregates generated during aerosolization and delivered through the airways. First, we screened the potency of IgG aggregates generated by nebulization to activate APC *in vitro*, using a standard human monocyte-derived dendritic cell (MoDC) assay. To take into consideration the complexity of the immune system and the lung mucosal environment, we evaluated the impact of nebulization-mediated IgG aggregates on immune cells *in vivo* after pulmonary administration. Our findings show that aggregation attributable to Ab nebulization induced immune cell activation, in a dose-dependent manner and delivering high-level of aggregates through the pulmonary route had a dramatic effect on immune cell homeostasis but also that this was avoidable through appropriate formulation approaches.

2. Materials and Methods

Mice

94 Adult male C57BL/6j (B6) mice (5 to 7 weeks old) were obtained from Janvier
95 (France). All mice were housed under specific-pathogen-free conditions at the PST
96 Animaleries animal facility (France) and had access to food and water ad libitum. All
97 animal experiments complied with the current European legislative, regulatory and eth-
98 ical requirements and were approved by the local animal care and use committee (ref-
99 erence: APAFIS#10200-2017061311352787).

100 Antibodies

101 Abs 1, 2 and 3 are full-length IgG1 (named hIgG1-1, hIgG1-2, hIgG1-3) used in the
102 clinics, supplied in their commercial formulation with endotoxin levels meeting ac-
103 ceptance thresholds (according to their certificate of analysis). To avoid any interference
104 on the aggregation propensity of each Ab, excipients were removed by hydroxyapatite
105 chromatography and subsequent dialysis against phosphate-buffered saline (PBS). Pro-
106 tein concentration was then evaluated for each Ab: hIgG1-1 [1.7mg/mL], hIgG1-2
107 [1.9mg/mL], hIgG1-3 [2.38mg/mL]

108 mAb166 (mIgG2b-1) is a murine monoclonal IgG2b, κ Ab against pcrV, a component
109 of a type three secretion system (T3SS) of *P. aeruginosa* [25]. MPC11 (mIgG2b-2) is the
110 control isotype of mAb166. Both were supplied as sterile, pyrogen-free solution in
111 phosphate-buffered saline (PBS), in accordance with good manufacturing practice, by
112 BioXcell (USA) with endotoxin level < 1 EU/ml (according to their certificate of analysis).
113 They were supplied as follows: mIgG2b-1 [2.5mg/mL], mIgG2b-2 [8.5mg/mL]. In some
114 experiments, Ab formulations were supplemented with Polysorbate 80 (Sigma-Aldrich,
115 France) at 0.01 or 0.05% (final volume) prior to nebulization.
116

117 Antibody nebulization

118 For sterility purposes, this procedure was performed under a cell-culture hood. All
119 antibodies, in suspension were filtered on a 0.22 μ m syringe filter (Millipore, France). For
120 *in vitro* assay, all antibodies were diluted in PBS1X to a final concentration of ~1.7 mg/mL
121 before nebulization. For each Ab, 1 mL were nebulized using a clinically used Aeroneb
122 Pro™ vibrating-mesh nebulizer (Aerogen, Ireland), connected with a 13 mL polypro-
123 pylene tube (Dutscher, France) or the VITROCELL Cloud 12 system (VITROCELL Sys-
124 tems, Germany), which is the commercial version of the Air-Liquid Interface Cell Ex-
125 posure-Cloud (ALICE-cloud) system, described by Lenz and colleagues [26]. Nebuliza-
126 tion duration was measured and lasted ~5min for each sample (i.e., 0.4 ml/min liquid
127 output rate). For *in vitro* aerosol-cell exposures, using the VITROCELL Cloud 12 system,
128 the aerosol cloud was allowed to settle for 20min before removing cells. When necessary,
129 nebulized Ab solutions were filtered on a 0.45 μ m syringe filter (Millipore, France) prior
130 to further analysis. Nebulizers were washed extensively between each nebulization ses-
131 sion using 0.22 μ m autoclaved water and PBS. Subsequently, nebulized PBS was analyzed
132 by flow cell microscopy and the nebulizer was considered cleaned and operating for Ab
133 nebulization when the nebulized PBS samples contained less than 300 particles/mL. To
134 rule out that cell activation may be attributable to contamination released during nebu-
135 lization, the activation potency of nebulized PBS (vehicle solution) was also investigated
136 *in vitro*. Our analysis revealed that nebulized PBS had no impact on MoDC activation
137 (data not shown).
138

139 Dynamic Light Scattering (DLS) analysis of antibodies

140 Native and nebulized Ab were analyzed by dynamic light scattering with a Dynapro
141 Nanostar® (Wyatt Technology, USA) after appropriate dilution to 100 μ g/ml in PBS1X1X
142 in UVette (Eppendorf, France). For each sample, the acquisition was performed 10 times
143 for 7 seconds each, at a temperature of 25°C with a detection angle of 90°. Particle diam-
144 eter (nm) and polydispersion index (pdi) were analyzed using Dynamics™ software
145 (Wyatt Technology, USA). Samples with less than 70% of successful analyses were con-
146

147 sidered multimodal and non-analyzable as recommended by the manufacturer (depicted
148 as n/a).

149 Flow cell microscopy (FCM) of antibodies

150 Native and nebulized Ab were analyzed by flow cell microscopy with an Occhio®
151 FC200S+ (Occhio, Belgium) after appropriate dilution to 100 µg/ml in medium in the
152 flowcell. Briefly, 250 µL of each antibody solution passed continuously in the flow cell,
153 where particles were automatically detected, sized and counted by a camera. Particle
154 counting, size assessment and distribution were analyzed using Callisto™ software
155 (Occhio, France).

156 Monocyte-derived dendritic cells (MoDC) preparation

157 Human peripheral mononuclear cells (PBMC) were purified from cytopheresis, ob-
158 tained from naïve donors (Etablissement Français du Sang, Hôpital Bretonneau, France)
159 by centrifugation on a Ficoll density gradient (Eurobio, France). MoDC were prepared
160 from PMBC as previously described [27]. Briefly, CD14+ monocytes were isolated using
161 magnetic cell sorting (Miltenyi Biotec, Germany) and cultured during 6 days, at
162 1x10⁶cells/mL in RPMI1640-Glutamax™ (Gibco, France) supplemented with 10% of
163 FCS (Dutscher, France), 1X Penicillin/Streptomycin (Gibco, France) in the presence of
164 25ng/mL of IL-4 (Miltenyi Biotec, Germany) and 100 ng/mL of GM-CSF. On day 6, ho-
165 mogeneity and viability of MoDC population was checked by flow cytometry based on
166 their physical characteristics (forward scatter (FSC) and side scatter (SSC)) and incorpo-
167 ration of vital dye (LiveDead™, Invitrogen, France). The immature phenotype of MoDC
168 was checked based on their DC-SIGN+, CD80^{low}, CD83^{low} and HLA-DR^{low} pheno-
169 type.

170 MoDC stimulation with antibody preparation

171 On day 6, immature MoDC were harvested and washed in complete medium
172 (RPMI1640-Glutamax™ supplemented with 10% of FCS (Dutscher, France) and 1X Peni-
173 cillin/Streptomycin). For experiments using Ab aerosols collected in a 13 mL polypro-
174 pylene tube, 1x10⁵cells/well were plated in 75µL in a U-bottom 96-well plate (Falcon,
175 BectonDickinson, France) for 4 hours. 75µL of nebulized or native Ab were then added to
176 a final concentration of 1, 10, 100 and 200 µg/mL depending on the experiments. For ex-
177 periments using the VITROCELL Cloud 12 system, 1x10⁵cells/well were plated in 150µL
178 on a 24-well plate permeable insert (Corning, France) for 18 hours. 200µL of complete
179 was added in the basolateral compartment to prevent cell drying. The insert was then
180 placed in the VITROCELL Cloud 12 system with 200µL in the basolateral compartment
181 and cells were exposed to Ab aerosol as describe above. Inserts were put back on a
182 companion 24-well plate.

183 Cells were incubated for 18 hours at 37°C with 5% CO₂. Lipopolysaccharide (LPS,
184 from Escherichia coli O111:B5, Sigma-Aldrich, France) was used at 1µg/mL as a positive
185 control. Untreated and nebulized PBS1X (Gibco, France) were used as vehicle controls.
186 Each condition was tested in 3-9 replicates.

187 Analysis of MoDC activation by flow cytometry

188 After 18 hours of stimulation, MoDC were harvested and saturated in PBS1X sup-
189 plemented with 2% of FCS, 2 mM EDTA and 1X of human Fc-Block (Becton Dickinson,
190 France) for 15 min at 4°C. Cells were washed and stained in FACS buffer (PBS1X sup-
191 plemented with 2% FCS and 2 mM EDTA) with antibodies described in Supplementary
192 table 2, for 20min at 4°C in the dark. Negative FMO controls were generated for each
193 parameter analyzed. All antibodies were from Biolegend (UK). Data acquisition was
194 made on the 8-colors MACSQuant flow cytometer (Miltenyi Biotec, Germany) on a
195 minimum of 10,000 living cells. MoDC analysis was performed using VenturiOne soft-
196 ware (Applied Cytometry, USA). Analysis was made on singlet (FSC-A / FSC-H gating)

and CD45+ live cells (negative for LiveDead staining). Costimulatory protein expression was expressed as a ratio of the median fluorescence intensity (MFI) of cells treated with nebulized Ab / MFI of cells treated with native Ab.

Cytokine, chemokine and protein assays

All assays were performed on Immulon™ 96-well plates (ThermoFischer, France). Concentrations of CXCL8 (IL-8), human IL-6 in cell-free MoDC supernatants and TNF, IL6, IL1b and CXCL1 (KC) were measured using specific ELISAs (Biolegend, UK; limit of detection: at 15.6 pg/mL) according to the manufacturer's instructions and were normalized based on the mean concentration of total protein. Total protein concentration was determined using a BCA assay (ThermoFischer Scientific, France), according to the manufacturer's instructions (limit of detection: 15 µg/mL).

Animal experiments

Animal experiments have been performed 2-3 times. For each experiments, 5 mice per groups were used. Nebulized or native mIgG2b-1 and mIgG2b-2 (100 µg/animal, in 40µL) were administered orotracheally or through intravenous injection using a restraining tube at days 0, 7, 14, 21 and 28. For orotracheal administration, mice were anesthetized with isoflurane 4% and an operating otoscope fit with intubation specula was introduced to both to maintain tongue retraction and to visualize the glottis. A fiber optic wire threaded through a 20G catheter and connected to torch stylet (Harvard Apparatus, France) was inserted into the mouse trachea. Correct intubation was confirmed using lung inflation bulb test and 40µL of the bacterial solution was applied using an ultrafine pipette tip. For the acute treatment assessment, animals were euthanized using a lethal dose of ketamine/xylazine at 4 hours, 1 day and 14 days after a single administration. In the chronic treatment groups, animals were euthanized at day 29.

At the time of necropsy, blood was recovered by intracardiac puncture. Bronchoalveolar lavage fluid (BALF) was then collected by cannulating the trachea and washing the lung twice with 1.2 mL of PBS1X at room temperature. The lavage fluid was centrifuged at 400 g for 10 min at 4°C, and the supernatant was stored at -20°C until analysis. The cell pellet was resuspended in FACS buffer and counted in a hemocytometer chamber. Peripheral blood was washed out by intracardiac perfusion with 10 mL of PBS1X. Lung and spleen homogenates were then prepared in 2mL of RPMI1640 containing 125 µg/mL of Liberase (Sigma-Aldrich, France) and 100 µg/mL of DnaseI (Sigma-Aldrich, France) using a GentleMACS tissue homogenizer (Miltenyi Biotec, Germany). Cells were isolated through a 100µm cell strainer and purified with a 20% Percoll (GE Healthcare, France) density gradient. Cell preparation was centrifuged at 400 g for 10 min at 4°C, and the pellet was resuspended in FACS buffer, and counted in a hemocytometer chamber.

Immune cell phenotyping by flow cytometry

BALF, lung and spleen cells isolated as described above were saturated in PBS1X supplemented with 2% of FCS, 2 mM EDTA and 1X of human Fc-Block (BectonDickinson, France) for 15 min at 4°C. Cells were washed and stained with antibodies described in Supplementary table 2 for 20min at 4°C in the dark. Data acquisition was made on the 8-colors MACSQuant flow cytometer (Miltenyi Biotec, Germany) on a minimum of 100,000 living cells. Analysis was performed using VenturiOne software (Applied Cytometry, USA). Analysis was made on singlet (FSC-A / FSC-H gating) and CD45+ live cells (negative for LiveDead staining). Immune cell phenotypes were determined as described in the Supplementary table 2. Data were normalized based on the mean concentration of respective native Ab conditions or expressed as a number of cell calculated as follow: % of the total CD45+ immune cell population x total number of cell. For Annexin-V/PI staining, data were normalized as follows: % of the positive population for nebulized Ab / % of the positive population for native Ab.

Histology

Lungs were fixed in 10% buffered formalin (Shandon), dehydrated in ethanol and embedded in paraffin. Serial sections (3 mm) were stained with haematoxylin and eosin (HE) or Congo Red. Ten HE sections per mouse were randomly evaluated to count cell nucleus using a machine-learning pixel classification plugin for Image J (<https://imagej.net/plugins/tws/>), as described previously [28].

Statistical analysis

Differences between experimental groups were determined using Kruskal-Wallis or t-test comparing two groups, using one or two-way analysis of variance (ANOVA) followed by Newman-Keuls or Bonferroni post-test (for comparison between more than two groups), after confirmation that the data were normally distributed. All statistical tests were performed with GraphPad Prism software (version 4.03 for Windows, GraphPad Software Inc., USA). All data are presented as mean \pm standard error of the mean (SEM). The threshold for statistical significance was set to $p < 0.05$.

3. Results

3.1. Aggregation of antibodies is heterogeneous during nebulization

Nebulization promotes Ab aggregation [10,11]. In this study, mesh-nebulization was used since it is less deleterious on Ab and often considered for aerosolization of proteins [5]. Full-length Ab commercially available or under preclinical development were reformulated in PBS and nebulized with the Aeronex Pro™ vibrating-mesh nebulizer.

Ab aggregation results in a broad range of particles, from dimers (several nanometers) to micron-sized, and even visible particles in some cases [29], requiring the combination of different complementary analytical techniques. The aggregation profiles of Ab were assessed using DLS and FCM to report particles at the submicrometric and micrometric scales, respectively (Figure 1).

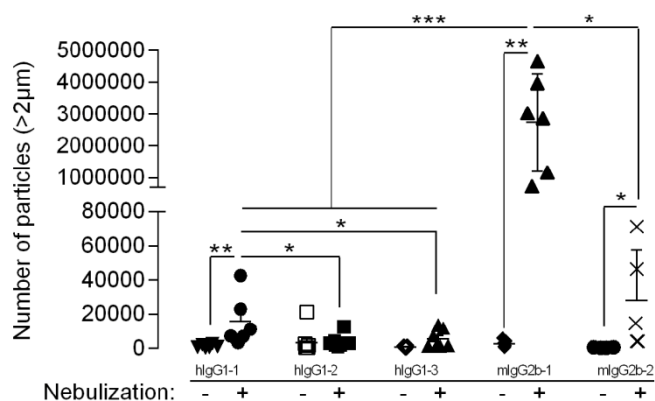


Figure 1. Antibodies were either nebulized using an Aeronex Pro™ vibrating-mesh nebulizer and collected (Nebulization +) or left untreated (Nebulization -). The total number of particles (with diameter $> 2 \mu\text{m}$) was quantified using a flow microscope. The data are quoted as the mean \pm SEM. *, **: $p < 0.05$, and $p < 0.01$ respectively, in a one-way ANOVA with Newman-Keuls's correction for multiple comparisons. The results represent three to eight independent nebulizations.

Nebulization led to an increase in the concentration of particles $> 2 \mu\text{m}$ for hlgG1-1, mlgG2b-1 and mlgG2b-2, as compared to their native counterparts. Conversely, no significant increase in particles was observed for hlgG1-2, hlgG1-3 (Figure 1). Furthermore, comparing nebulized Ab, we observed that hlgG1-1 and mlgG2b-1 had significantly more particles than the other human and murine Ab, respectively. In addition to differences in total particle concentration, there were also differences in particle size distribu-

tion. Nebulized hlgG1-1 and -2 had more than 78% of their particles smaller than 5 μm , while hlgG1-3, mlgG2b-1 and mlgG2b-2 comprised more than 33% of their particles above 5 μm (Table 1). For murine mlgG2b-1 and mlgG2b-2, aggregation was also observed at the submicron scale, most notably for nebulized mlgG2b-1, which could not even be analyzed by DLS due to the large heterogeneity of the particle size distribution (most likely all-sized Ab aggregates), which cannot be clearly structured in defined size modes – a prerequisite for DLS measurements. Nebulized mlgG2b-2 exhibited a significant reduction (7%) of monomeric Ab amount (Supplementary Table 1). Overall, our results highlight the huge heterogeneity of Ab aggregation during mesh nebulization, most likely depending on Ab sequence/structure.

Table 1. Particle size distribution (%) of nebulized antibodies.

Antibody	2-5 μm	5-25 μm	>25 μm
hlgG1-1	84,3	14,7	1,1
hlgG1-2	78,4	21,1	0,4
hlgG1-3	53,8	45,8	0,4
mlgG2b-1	67,0	32,3	0,7
mlgG2b-2	57,8	40,7	1,6

3.2. Ab aggregates, produced during mesh-nebulization, activate antigen-presenting cells

The dramatic consequences of adverse immunogenicity have prompted regulatory authorities to establish a guidance to test the immunogenicity of therapeutic protein products and industry to propose screening approaches [30,31]. They include investigating the ability of protein aggregates to activate immune cells, *in vitro*.

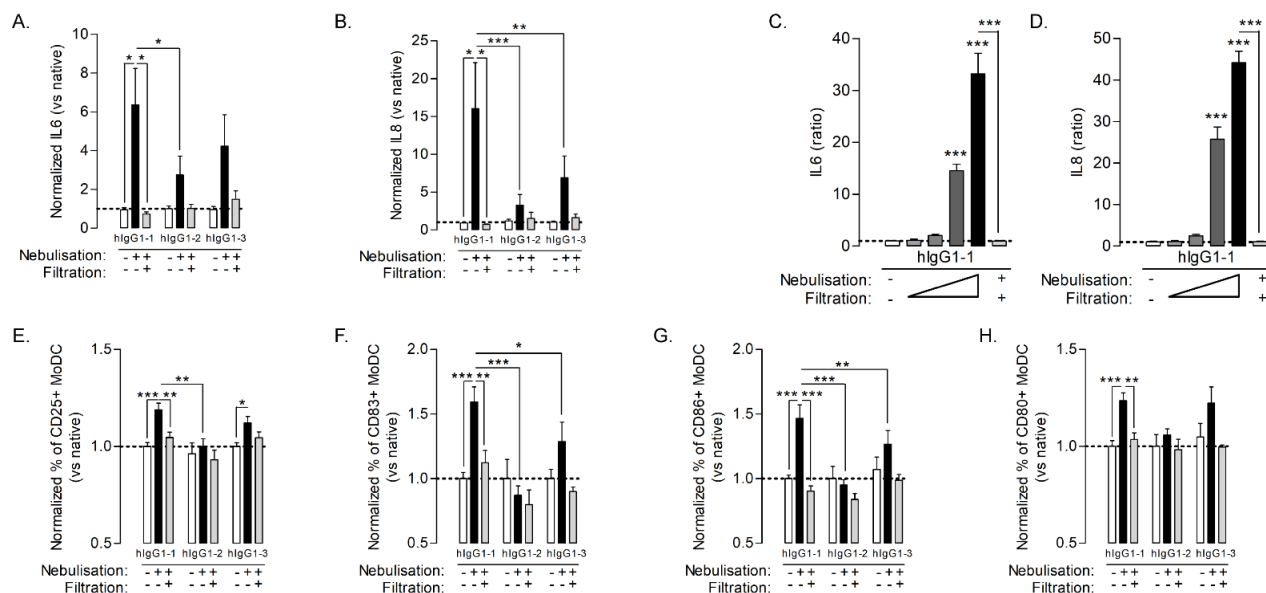


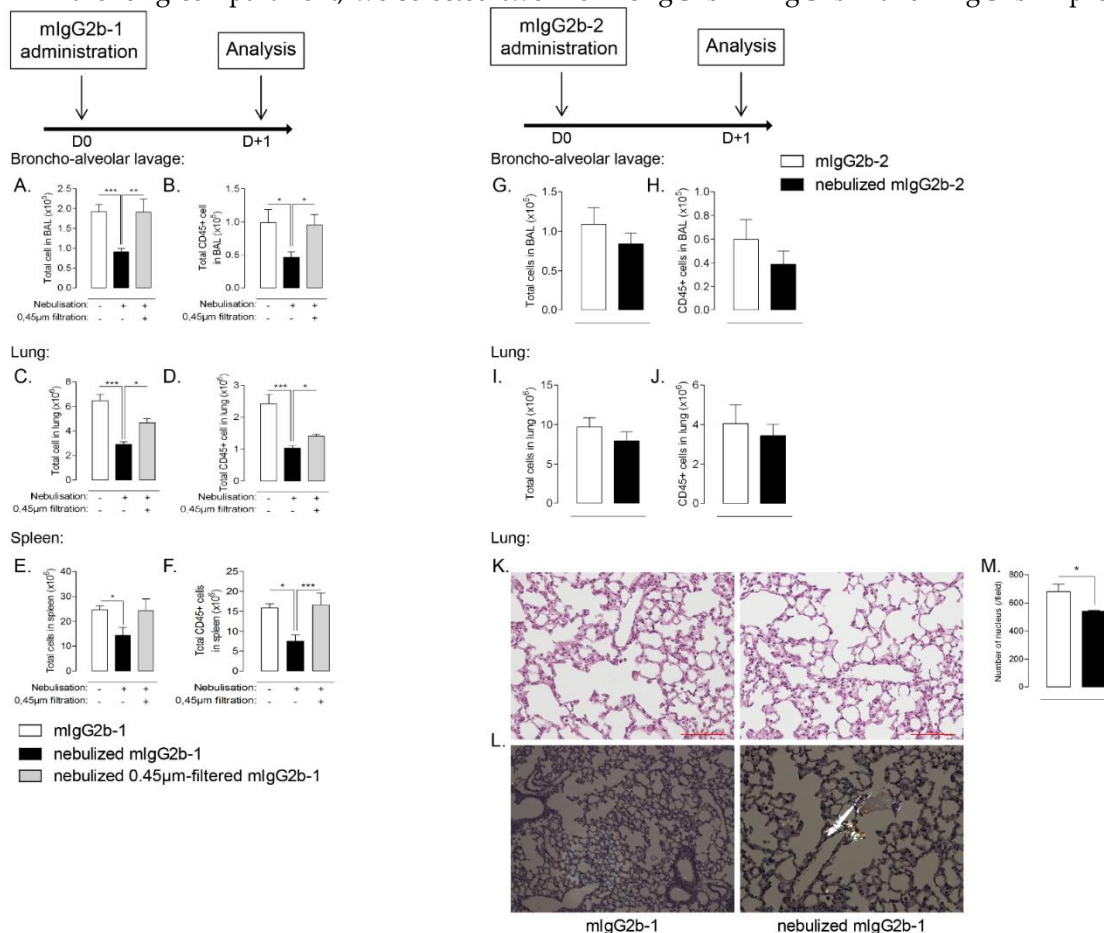
Figure 2. MoDC were stimulated using equal final concentration of Ab at 100 $\mu\text{g}/\text{mL}$ either native (white bars), nebulized (black bars) or nebulized and 0.45 μm -filtered (gray bars) for 18h. IL6 (A) and IL8 (B) were quantified in cell-free supernatant. MoDC were stimulated with 1, 10, 100 or 200 $\mu\text{g}/\text{mL}$ (gray to black bars) of nebulized hlgG1 or 100 $\mu\text{g}/\text{mL}$ of nebulized and 0.45 μm -filtered hlgG1 (last bar) or left untreated (white bars) for 18h. IL6 (C) and IL8 (D) were quantified in cell-free supernatant. MoDC were stimulated using equal final concentration of Ab at 100 $\mu\text{g}/\text{mL}$ either native (white bars), nebulized (black bars) or nebulized and 0.45 μm -filtered (gray bars) for 18h. CD25 (E), CD83 (F), CD86 (G), CD80 (H) expression were measured using flow cytometry. The data are quoted as the mean \pm SEM. *, **, ***: $p < 0.05$, $p < 0.01$ and $p < 0.001$ respectively, in a one-way ANOVA with Newman-Keuls's correction for multiple comparisons. The results are representative of six independent experiments ($n = 6-9$ technical replicates/experiment).

323 Here, we incubated human monocyte-derived dendritic cells (MoDC) overnight
324 with native or nebulized Abs (hIgG1-1 to -3) and analyzed both the release of
325 pro-inflammatory cytokines and expression of co-stimulatory proteins involved in the
326 DC-T synapse (CD25, CD83, CD86 and CD80). Neither the native Ab, nor the nebulized
327 buffer without Ab (data not shown) promoted IL-6 or IL-8 production by MoDC (Figures
328 2A and 2B) and modulated cell markers as compared to untreated MoDC (Figures 2E-H).
329 Nebulized and aggregated hIgG1-1 induced a significant and dose-dependent increase of
330 cytokine production (Figures 2A-D) whereas the other nebulized Ab solutions had only a
331 minor and inconsistent impact on cytokine level. The nebulized and aggregated hIgG1-1
332 induced a slight but significant increase in all cell markers, whereas the effect of other
333 nebulized Ab was limited (Figures 2E-H). Interestingly, the filtration of Ab solutions after
334 nebulization, removing micrometric particles (data not shown), resulted in the abroga-
335 tion of both cytokine release and expression of co-stimulatory markers by MoDC (Figures
336 2A-H, gray bars). In addition, when comparing nebulized antibodies, our analysis re-
337 vealed that activation potency of hIgG1-1 was higher than for hIgG1-2 and hIgG1-3. Al-
338 together, our results suggest that activation of APC was attributable to the presence of
339 aggregates and that the extent of this activation was correlated to the number of particles
340 (Figure 1). Since aerosol collection system may modulate the amount and the size dis-
341 tribution of Ab aggregates after nebulization [11], we determined whether collection
342 might induce a bias in APC activation. We exposed directly MoDC to hIgG1-1 aerosols
343 using the VITROCELL Cloud 12 system [26]. As observed in Supplementary Figure 1, we
344 obtained similar results on MoDC activation independent of whether the cells were di-
345 rectly exposed to hIgG1-1 aerosols (through use of the VITROCELL Cloud 12 system) or
346 exposed to them after collection as a bulk solution supporting our decision of adopting
347 the latter approach. Taken together, our results showed that nebulized Ab induced
348 MoDC maturation and activation as compared to native Ab, and confirmed the in-
349 volvement of Ab aggregates in this response.
350

351 3.3. High-level of nebulization-mediated antibody aggregates impair lung cell homeostasis after 352 lung delivery

353
354
355
356
357
358

Historically, *in vitro* assays have been widely used to describe the potential immunogenicity of biotherapeutic aggregates [13]. However, they display several limitations: (i) the amount of aggregates inducing a response *in vitro* may not directly translate into *in vivo* response and (ii) they may not predict the impact of the pulmonary delivery route. To gain insight into the broad effects of Ab aggregates produced by aerosolization within the lung compartment, we selected two murine IgG2b – mIgG2b-1 and mIgG2b-2-

359
360
361
362
363
364
365
366
367
368
369

ducing different amounts of aggregates during mesh-nebulization (Figure 1) which differentially activate MoDC (Supplementary figures 2). We administered them through the airways in naïve mice. Remarkably, the nebulized and aggregated mIgG2b-1 resulted in a dramatic reduction in the total cell number in the airway compartment of mice (BAL), as compared to native antibodies administered by the same route (Figure 3A). Moreover, nebulized mIgG2b-2, producing 10-fold less aggregates after mesh-nebulization than mIgG2b-1 (Figure 1), showed no statistically significant reduction in BAL cell number (Figures 3G). Of note, the animals that received the native Ab through the airways had similar cell count as sham animals (data not shown), which implies that the oro-tracheal application itself did not obfuscate our results.

370
371
372
373
374
375
376
377
378

Figure 3. B6 mice received a 40 μ L orotracheal instillation of mIgG2b-1 at 100 μ g/mL either native (white bars), nebulized (black bars) or nebulized and 0.45 μ m-filtered (gray bars). The total number of cells (A, C and E) and CD45⁺ cells (B, D and F) were quantified in BAL (A and B), in the lungs (C and D) and the spleen (E and F) using flow cytometry, 18h after the administration. B6 mice received a 40 μ L orotracheal instillation of mIgG2b-2 at 100 μ g/mL either native (white bars) or nebulized (black bars). The total number of cells (G and I) and CD45⁺ cells (H and J) were quantified in BAL (G and H), in the lungs (I and J) using flow cytometry, 18h after the administration. Lung tissues of mice treated with either native (white bars) or nebulized (black bars) mIgG2b-1 were histologically examined 18h after the administration. (K) Hematoxylin-eosin sections were used to

379 quantify cell nucleus (M) by machine-learning (see material and methods section). (L) Congo-Red
380 sections were observed under polarized light. Aggregates are identified as apple-green birefrin-
381 gence artifacts.. 10 sections / mouse were observed at x20 magnification and used for ma-
382 chine-learning quantification. The data are quoted as the mean \pm SEM. *, **, *** : $p < 0.05$, $p < 0.01$ and
383 $p < 0.001$ respectively, in a one-way ANOVA with Newman-Keuls's correction for multiple com-
384 parisons. The results are representative of three independent experiments (n=5 mice/experiment).

385 Analysis of the cellular phenotype of the BAL cells revealed an analogous result for
386 immune (CD45+ leukocytes) cells (Figures 3B and 3H). Further analysis did not reveal
387 any impact on specific lineage as almost all immune cell lineages were affected after the
388 administration of aggregated Ab (Supplementary Figures 3A-E). In the lung tissue, ne-
389 bulized mIgG2b-1 caused a 2-fold reduction in total cell and leukocyte counts relative to
390 controls (Figures 3C-D), while nebulization of mIgG2b-2 did not modify leukocyte counts
391 (Figures 3I and J). This decrease affected both myeloid (neutrophil, monocyte, dendritic
392 cell) (Supplementary Figures 3F-I) and lymphoid lineages (B, T CD4+/CD8+ cells) (Sup-
393 plementary Figures 3J-L). The modification of cell homeostasis in the airway compart-
394 ment was not associated with an alteration of the lung epithelial barrier (Supplementary
395 figure 4), but was mostly attributable to micron-sized particles as 0.45 μ m-filtration of
396 nebulized mIgG2b-1 prevented these adverse effects (Figures 3A-F, gray bars). The fil-
397 tration step did not significantly modify Ab particle size distribution (Supplementary
398 Tables 4 and 5) or concentration (Supplementary Table 6), as compared to native Ab.

399 Interestingly, we observed protein aggregates (appearing as apple-green birefrin-
400 gence structures under polarized light) on Congo-red stained lung sections from animals
401 treated with nebulized mIgG2b-1 (Figure 3L). Unsupervised machine learning, which
402 was used to quantify cell nucleus on HE-stained lung section, showed that local admin-
403 istration of nebulized mIgG2b-1 was associated with a significant reduction of lung cells
404 after 18 hours (Figures 3K and 3M). Unexpectedly, the number of total and immune cells
405 was also diminished, even though to a lesser extent, in the spleen (Figures 3E-F), indi-
406 cating that the impairment of cellular homeostasis reached the systemic compartment.
407 Contraction of cell number 18h after a single airway administration of nebulized Ab
408 primarily occurred in the airways, and then probably extended through the lung tissue
409 and systemically as it was restricted to the airway compartment after 4 hours (Figures
410 4A-4F). Moreover, this effect was sustained for at least up to 14 days after Ab admin-
411 istration (Figures 4G and 4H), or after repeated administrations (Figures 4I-4N). For ei-
412 ther single or repeated administrations of nebulized mIg2b-1, we did not observe any
413 sign of general toxicity, including body-weight loss (data not shown). Overall, our results
414 suggest that airway administration of aggregated IgG (>0.45 μ m) profoundly affected
415 cellular homeostasis, in a time-dependent manner, both locally and systemically.

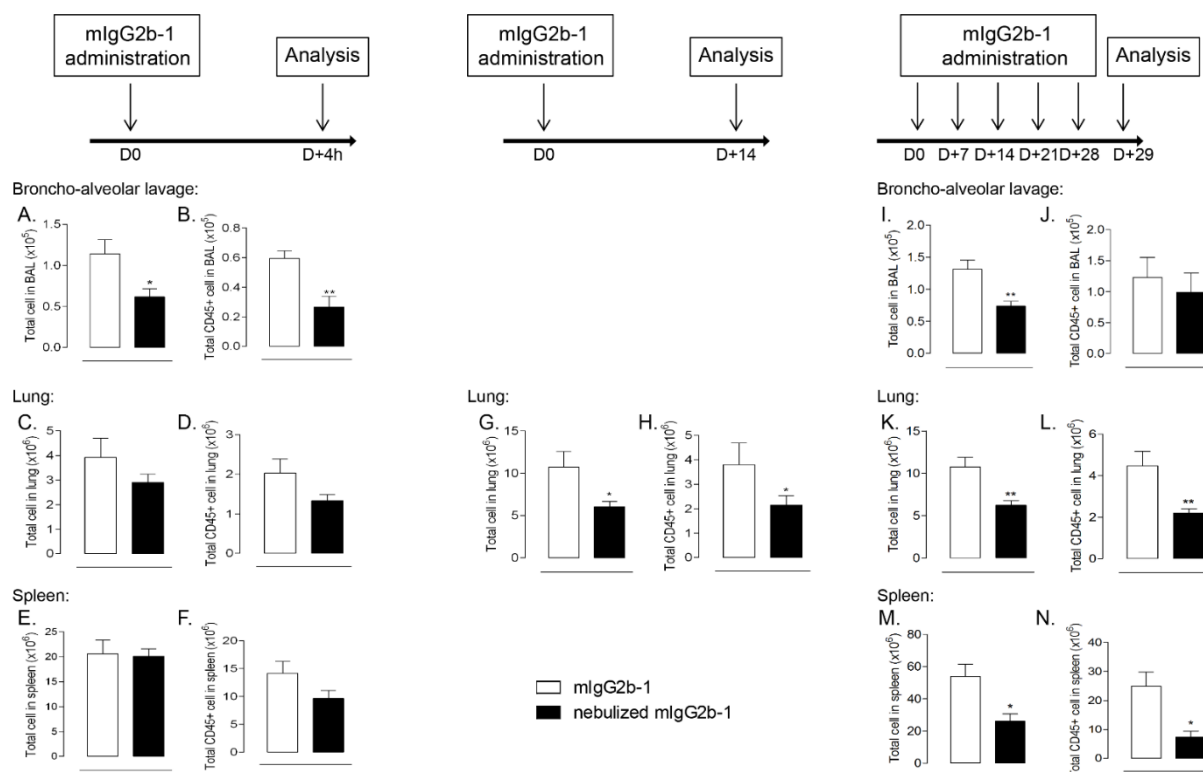


Figure 4. B6 mice received a 40 μ L orotracheal instillation of mIg2b-1 at 100 μ g/mL either native (white bars) or nebulized (black bars) through the airways at D0, or D+0, D+7, D+14, D+21 and D+28. The total number of cells (A, C, E, G, I, K and M) and CD45+ cells (B, D, F, H, J, L and N) were quantified in BAL (A, B, I and J), in the lungs (C, D, G, H, K and L) and the spleen (E, F, M and N) using flow cytometry, 4h, 14 days or 29 days after the first administration. The data are quoted as the mean \pm SEM. *, **: $p < 0.05$ and $p < 0.01$ respectively, in a t-test. The results are representative of two independent experiments ($n = 5$ mice /experiment).

3.4. Nebulized aggregated antibody induced immunologically silent cell death after lung administration

Next, we investigated the mechanisms accounting for host cell contraction and hypothesized that it was associated with cell death. Cell death occurs in multiple forms and can be divided in accidental cell death (ACD; necrosis) or regulated cell death (RCD; apoptosis) [32]. ACD is characterized by a dramatic and instantaneous collapse of cells and can be triggered in response to different stresses, including chemical, physical or mechanical insults, whereas RCD relies on committed molecular machinery [33]. Using Annexin-V/propidium iodide (PI) staining, which allows the discrimination of early apoptotic cells (Annexin-V+/PI-), late apoptotic cells (Annexin-V+/PI+) and necrotic cells (Annexin-V-/PI+) [34], we quantified the proportion of each cell death phenotypes in both total cells and CD45+ leukocytes population, 18 hours after a single administration of mIgG2b-1. We observed that administration of nebulized mIgG2b-1 provoked a significant increase of both late apoptotic and necrotic spleen cells while lung and airway cells were suffering from necrosis, as compared to mice treated with native Ab (Figures 5A-5F) or with nebulized mIgG2b-2 (Supplementary Figure 5). The type of cell death could also be determined by the analysis of mediators released in the environment. When comparing BALs from animals treated with native and nebulized mIgG2b-1, we did not observe any significant difference in the production of TNF, IL-6, IL-1b or CXCL1 (KC) (Figures 5G-J). These data suggested that the cell contraction occurring after single or multiple airway administration of nebulized and aggregated IgG was associated with an inflammatory silent cell death process.

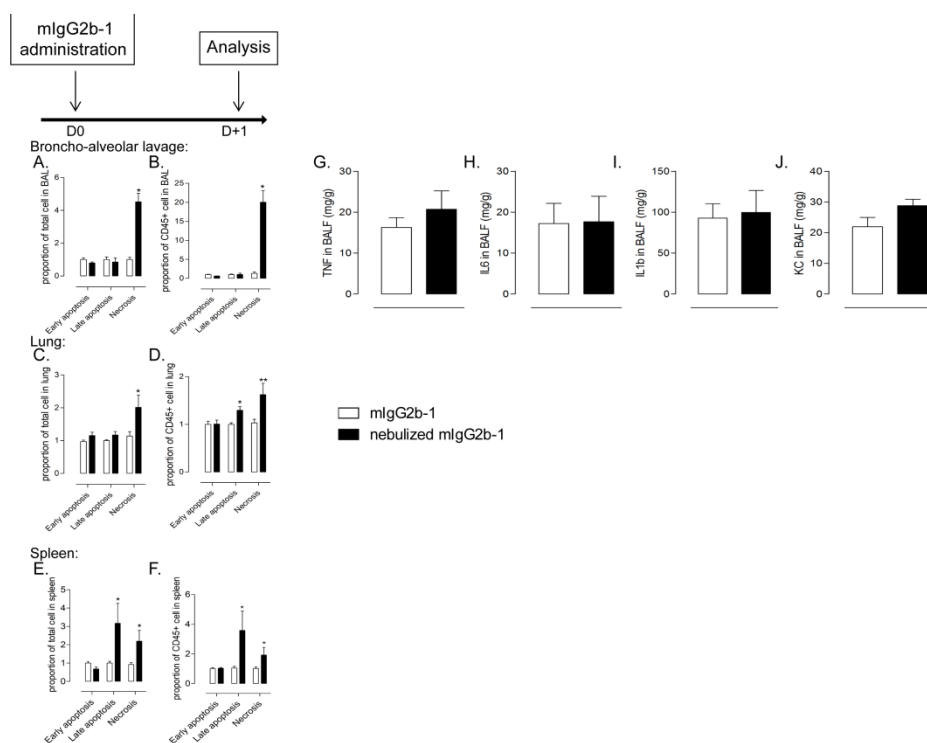


Figure 5. B6 mice received a single 40 μ L orotracheal instillation of mIg2b-1 at 100 μ g/mL either native (white bars) or nebulized (black bars). The proportion of early apoptotic cells (Annexin-V+/PI-), late apoptotic cells (Annexin-V+/PI+) and necrotic cells (Annexin-V-/PI+) were quantified in total cell (A, C and E) or CD45+ cell (B, D and F), 18h after the administration in BAL (A and B), lungs (C and D) and spleen (E and F) relative to mice treated with native Ab using flow cytometry. The concentrations of TNF (G), IL6 (H), IL1b (I) and KC (J) in BALF were determined 18h after the administration. The data are quoted as the mean \pm SEM. *, **: $p < 0.05$ and $p < 0.01$ respectively, in a t-test. The results are representative of three independent experiments (n=5 mice/experiment).

3.5. The effect of nebulization-mediated antibody aggregates on immune cell homeostasis is specific of the pulmonary route

Immunogenicity of Ab is also dependent of their route of administration [20-22]. Thus, we investigated the effect of native or nebulized-mIgG2b-1 after intravenous injection. In contrast to what was observed after airway administration, there were no significant differences in the BAL or lung cell counts in the animals who received native or nebulized mIgG2b-1 intravenously (Figures 6A-6D). Interestingly, these results were substantiated when analyzing cell number after repeated administration of nebulized mIgG2b-1 (Supplementary Figure 6), where no differences were noticed in the airways or lungs of animals treated by repeated intravenous injections as compared to animals, which received the IgG in the lungs. Our data suggested that the route of administration played an important role on the adverse effect of IgG aggregates produced during nebulization on cell homeostasis.

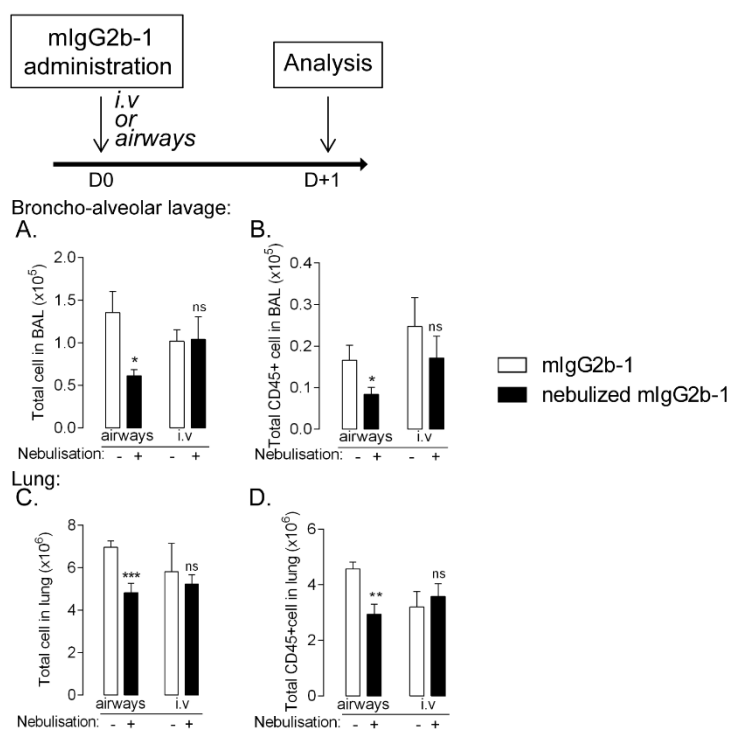


Figure 6. B6 mice received a 40 μ L orotracheal instillation or 100 μ L intravenous injection of mIgG2b-1 at 100 μ g/mL either native (white bars) or nebulized (black bars). The total number of cells (A and C) and CD45+ cells (B and D) were quantified in BAL (A and B) and in the lungs (C and D) using flow cytometry, 18h after the administration. The data are quoted as the mean \pm SEM. *, **, ***: $p < 0.05$, $p < 0.01$ and $p < 0.001$ respectively, in a t-test. The results are representative of two independent experiments (n=5 mice/experiment).

3.6. Reducing aggregation limits pulmonary cytotoxicity associated to lung administration of nebulized Ab

Pharmaceutical development aims to design a high-quality product ensuring an efficacious and safe treatment along the life of the product. Hence, formulation and protein engineering are often adapted to limit Ab aggregation, especially considering chronic-based therapies. Different parameters, including addition of surfactant, have a protective effect, limiting Ab aggregation during nebulization [10]. Here, we added polysorbate80 (PS80) in mIgG2b-1 formulation to significantly reduce its aggregation during nebulization (Supplementary Figure 7). The addition of surfactant did not significantly modify Ab particle size distribution (Supplementary Tables 4 and 5) or concentration (Supplementary Table 6) as compared to unformulated Ab. Single administration of nebulized mIgG2b-1 supplemented with 0,05% of PS80 abrogated the reduction of lung cell number (Figures 7C and D) and to a lesser extent of airway cell (Figures 7A and B) as compared to non-formulated mIgG2b-1. This was likely attributable with a reduction of cell death in the same compartment (Supplementary Figure 8). These results suggest that optimizing IgG formulation improved its molecular stability and might limit adverse effects on cell homeostasis.

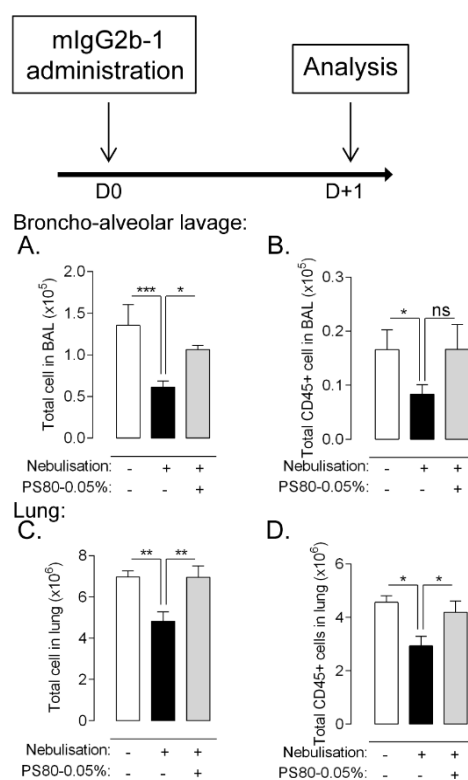


Figure 7. B6 mice received a 40 μ L orotracheal instillation of mIgG2b-1 at 100 μ g/mL either native (white bars), nebulized (black bars) or nebulized + Polysorbate80 0.05% (PS80 0.05%, gray bars). The total number of cells (A and C) and CD45+ cells (B and D) were quantified in BAL (A and B) and in the lungs (C and D) using flow cytometry, 18h after the administration. The data are quoted as the mean \pm SEM. *, **, ***: $p < 0.05$, $p < 0.01$ and $p < 0.001$ respectively, in a t-test. The results are representative of two independent experiments ($n = 5$ mice/experiment).

4. Discussion

Ab are highly sensitive to stresses encountered during their product development, manufacturing, storage or clinical use, and they often require high therapeutic doses, necessitating high concentration drug products with a higher risk of aggregation. Tracking aggregates prior and after Ab bioprocessing is essential to avoid risks for patients, treatment failure and ultimately termination of drug development/commercialization.

Protein aggregation has been widely demonstrated as an influential factor in the induction of adverse immunogenicity of biotherapeutics [35,36]. However, some of the stress conditions used in the literature are not representative of those experienced during product development, manufacturing, storage or clinical use, making the aggregates generated far different from those found in marketed products. This may hamper conclusions about the exact potency of protein aggregation in the occurrence of drug immunogenicity. Several intrinsic or extrinsic attributes of aggregates might work synergistically to induce immunogenicity. Among them, parameters related to the delivery route can affect the immune response associated with the administration of drugs. For example, subcutaneous delivery has been associated with higher immunogenicity than the intravenous route, for several biotherapeutics [37,38]. To our knowledge, there is not any study conducted so far to assess the immunogenicity associated with lung administration of an aerosolized and aggregated Ab. We set out a dual experimental approach to investigate the quality and the extent of the immune responses induced by a nebulized and aggregated Ab using both *in vitro* and *in vivo* models. Here, we showed for the first time that the aggregates resulting from IgG nebulization induced immune cell

527 over-activation and that their delivery to the lung markedly and durably impaired cell
528 homeostasis.

529 Protein aggregation is a process of non-specific association of monomers through
530 multiple physical and chemical pathways which are well documented [39]. The charac-
531 teristics of protein aggregates are variable in terms of particle size, number, morphology,
532 chemical modifications, reversibility, conformation or hydrophobicity [40]. This pheno-
533 typic heterogeneity results from the various stresses applied to proteins and require spe-
534 cific analytical methods [41]. Aerosol generation involves the dispersion of liquid drop-
535 lets into a gas. This process may be associated with physical stresses including tempera-
536 ture variations and the generation of a massive air-liquid interface, which ultimately in-
537 duce changes in protein conformation and lead to its aggregation [10]. We measured the
538 aggregation of several human IgG submitted to aerosolization using a vibrating-mesh
539 nebulizer, which is expected to be less deleterious than other nebulizers [42,43]. Flow cell
540 microscopy and dynamic light scattering revealed that the number and size of aggregates
541 were Ab dependent, confirming the results in the literature on the necessity of a
542 case-by-case approach. Besides, drastic differences were observed between commercial
543 Abs (hIgG1-1 to 3) and murine Abs (mIgG2b-1 and -2), where the latter displayed higher
544 aggregation upon nebulization. This may be explained by the fact that commercial Abs
545 underwent advanced development programs and were thus selected for their limited
546 aggregation potency. We next determined whether the aggregates found in the thera-
547 peutic product after nebulization may induce immunogenicity using a MoDC-based as-
548 say, which has been widely used to describe the potential immunogenicity of
549 biotherapeutics or unwanted products [44]. Our analysis revealed that nebulized and
550 aggregated hIgG1 – in particular hIgG1-1, were able to induce MoDC activation and
551 maturation, as evidenced by the enhanced secretion of cytokines and increased expres-
552 sion of co-stimulatory proteins on MoDC. This response correlated with the fraction of
553 micron-sized aggregates in the Ab aerosol. There are still discrepancies regarding the size
554 and type of aggregates involved in the generation of immunogenic responses [45]. This
555 depends on the type and strength of the stress applied and the multiple experimental
556 protocols which have been described [21,46]. Here, hIgG1-1 aerosol is mainly composed
557 of small-sized particles (2-10 μ m), which have been shown to enhance the immune re-
558 sponse and be the most immunogenic [45,47].

559 One potential bias regarding Ab aggregation could be attributed to the aerosol col-
560 lection step, which uses a polypropylene tube to re-pool aerosol droplets into a bulk liq-
561 uid. Indeed, it has been evidenced that the aerosol collection device could influence pro-
562 tein stability, generating different aggregation profiles [11,48]. In this context, we used
563 the VITROCELL technology, which was developed to improve reliability of toxicological
564 studies of aerosolized compounds on air-liquid interface cell cultures [49,50]. This sys-
565 tem, which allows direct deposition of aerosols on cells, avoids the collection step [51].
566 Our results showed that direct hIgG1-1 deposition on MoDCs resulted in cell activation,
567 as evidenced by the similar increase in both cytokine production and expression of
568 costimulatory proteins than those obtained with the nebulized-collected Ab. Thus, the
569 collection system used here was considered relevant for these assays and was kept for the
570 *in vivo* experiments.

571 To take into account the complexity of the lung mucosal-associated immune system,
572 it was necessary to use an animal model to predict the immunogenicity of nebulized Ab
573 *in vivo* [52,53]. We chose murine antibodies to avoid a high immunogenic background
574 response due to the non-specific activation of the mouse immune system by foreign
575 proteins. In our study, we observed that single or repeated administration of a nebulized
576 antibody in the lungs induced a significant contraction of the total and immune cell
577 number in the airways starting quickly after the administration as compared to native Ab
578 or saline controls. This was dependent on the number of aggregates as low aggregated
579 Ab, filtered or PS80 preparation of nebulized Ab did not have any impact on cell number.
580 Interestingly, at later time-points this contraction reached the lung parenchyma and the

spleen, reducing significantly the number of both myeloid and lymphoid cells. We wondered whether this cell number reduction induced by the administration of nebulized Ab was associated with cell death. We observed that apoptosis were significantly increased in lung total cells and in leukocytes after airway administration of nebulized Ab. Interestingly, these cellular injuries were dependent on the presence of aggregates, as Ab formulated with surfactant, known to limit aggregation [10], and even filtered nebulized Ab preparation did not promote cell death. These adverse effects were also dependent on the route of administration as nebulized Ab administered through the intravenous route was not associated with the same cell number reduction. The complete understanding of the molecular and cellular mechanism associated with the massive cytotoxicity of nebulized and aggregated antibodies requires further investigations.

Protein aggregation underlies many chronic diseases where aggregates are thought to elicit injury including cell apoptosis [54,55]. To the best of our knowledge, this is the first study reporting that extracellular therapeutic protein aggregates may sensitize the host to cytotoxicity. This cellular injury occurred in the absence of a pro-inflammatory response which is contradictory with the current paradigm regarding the induction of innate immune responses by protein aggregates [13]. This discrepancy may come from the attributes of Ab aggregates associated with nebulization, as compared to the ones associated with other aggregation stresses, including the formation of neoepitopes, the immunomodulatory properties of the aggregates, the exposure of post-translational modifications or the generation of danger signals [56]. A complete understanding of the physical mechanisms accounting for the immunogenic properties of nebulized Ab aggregates is beyond the scope of this study. Immunogenicity may also be associated with the breakdown of self-tolerance rather than an active immune response [56]. It is particularly concordant with repeated exposure which may occur during dosing regimen for chronic disease [36].

In conclusion, we demonstrated that aerosolization using a clinically relevant nebulizer induced Ab aggregation and resulted in immune cell activation and immunocytotoxicity *in vivo*. Although there are still many questions to address to understand better the relationship between Ab aggregates and immunogenicity, our findings point a significant role of the route of administration in the immunogenic/biological response associated to Ab aggregates. Further investigations will be required to determine the types and the amount of aggregates and the role of the Fc domain in the immunocytotoxic response of Ab aggregates produced during nebulization. Our findings also highlight the importance to explore further the different methods (protein engineering, aerosolization process, formulations) to stabilize further Ab during aerosolization to minimize risks for the patients.

Supplementary Materials: The following supporting information can be downloaded at: www.mdpi.com/xxx/s1, Figure S1: *in vitro* aerosol-MoDC exposure using Vitrocell; Figure S2: MoDC activation by nebulized mIgG2b-1; Figure S3: Lung cell immunophenotyping after administration of nebulized mIgG2b-1; Figure S4: Protein content in BALF after administration of nebulized mIgG2b-1; Figure S5: Apoptosis of lung and airway cells after administration of nebulized mIgG2b-2; Figure S6: Lung and airway cell count after i.v administration of nebulized mIgG2b-1; Figure S7: Effect of PS80 on the generation of aggregate after mIgG2b-1 nebulization; Figure S8: Lung cell count after administration of nebulized mIgG2b-1 supplemented with PS80-0.05%; Table S1: Dynamic light scattering analysis of nebulized antibodies; Table S2: List of antibodies used for flow cytometry; Table S3: Phenotype of analyzed cells; Table S4: Particle size distribution (%) of nebulized antibodies; Table S5: Dynamic light scattering analysis of nebulized antibodies; Table S6: Nanodrop analysis of antibody concentration.

Author Contributions: TS and NHV conceived the study. All authors substantially contributed to the acquisition, analysis or interpretation of data. GI performed machine-learning analysis of histological sections. OS loaned the VITROCELL Cloud 12 system and provided expertise regarding the ALICE-cloud system. TS and NHV contributed to manuscript drafting, revising and critically reviewing. All authors approved the final version of this manuscript to be published.

Funding: This work was supported by a public grant overseen by the French National Research Agency (ANR) as part of the “Investissements d’Avenir” program (LabEx MAbImprove, ANR-10-LABX-53-01). TS is funded by a fellowship from ANR-10-LABX-53-01.

Data Availability Statement: The data supporting this article will be shared on reasonable request to the corresponding author.

Acknowledgments: We sincerely thank David Fraser PhD (Biotech Communication SARL, France) for copy-editing services and Dr. Roxane Lemoine (Université of Tours, EA4245) for providing MoDC.

Conflicts of Interest: NHV is co-founder and scientific expert for Cynbiose Respiratory. In the past two years, she received consultancy fees from Eli Lilly, Argenx, Novartis and research support from Sanofi and Aerogen Ltd. RML is Head of R&D, Science and Emerging Technologies in Aerogen. All other authors have no competing interests to declare.

References

1. Anselmo, A.C.; Gokarn, Y.; Mitragotri, S. Non-invasive delivery strategies for biologics. *Nature reviews. Drug discovery* 2019, 18, 19-40, doi:10.1038/nrd.2018.183.
2. Dall'Acqua, W.F.; Kiener, P.A.; Wu, H. Properties of human IgG1s engineered for enhanced binding to the neonatal Fc receptor (FcRn). *The Journal of biological chemistry* 2006, 281, 23514-23524, doi:10.1074/jbc.M604292200.
3. Hart, T.K.; Cook, R.M.; Zia-Amirhosseini, P.; Minthorn, E.; Sellers, T.S.; Maleeff, B.E.; Eustis, S.; Schwartz, L.W.; Tsui, P.; Appelbaum, E.R.; et al. Preclinical efficacy and safety of mepolizumab (SB-240563), a humanized monoclonal antibody to IL-5, in cynomolgus monkeys. *The Journal of allergy and clinical immunology* 2001, 108, 250-257, doi:10.1067/mai.2001.116576.
4. Koleba, T.; Ensom, M.H. Pharmacokinetics of intravenous immunoglobulin: a systematic review. *Pharmacotherapy* 2006, 26, 813-827, doi:10.1592/phco.26.6.813.
5. Bodier-Montagutelli, E.; Mayor, A.; Vecellio, L.; Respaud, R.; Heuze-Vourc'h, N. Designing inhaled protein therapeutics for topical lung delivery: what are the next steps? *Expert opinion on drug delivery* 2018, 15, 729-736, doi:10.1080/17425247.2018.1503251.
6. Secher, T.; Dalonneau, E.; Ferreira, M.; Parent, C.; Azzopardi, N.; Paintaud, G.; Si-Tahar, M.; Heuze-Vourc'h, N. In a murine model of acute lung infection, airway administration of a therapeutic antibody confers greater protection than parenteral administration. *Journal of controlled release : official journal of the Controlled Release Society* 2019, 303, 24-33, doi:10.1016/j.jconrel.2019.04.005.
7. Secher, T.; Mayor, A.; Heuze-Vourc'h, N. Inhalation of Immuno-Therapeutics/-Prophylactics to Fight Respiratory Tract Infections: An Appropriate Drug at the Right Place! *Frontiers in immunology* 2019, 10, 2760, doi:10.3389/fimmu.2019.02760.
8. Depreter, F.; Pilcer, G.; Amighi, K. Inhaled proteins: challenges and perspectives. *International journal of pharmaceutics* 2013, 447, 251-280, doi:10.1016/j.ijpharm.2013.02.031.
9. Hertel, S.P.; Winter, G.; Friess, W. Protein stability in pulmonary drug delivery via nebulization. *Advanced drug delivery reviews* 2015, 93, 79-94, doi:10.1016/j.addr.2014.10.003.
10. Respaud, R.; Marchand, D.; Parent, C.; Pelat, T.; Thullier, P.; Tournamille, J.F.; Viaud-Massuard, M.C.; Diot, P.; Si-Tahar, M.; Vecellio, L.; et al. Effect of formulation on the stability and aerosol performance of a nebulized antibody. *mAbs* 2014, 6, 1347-1355, doi:10.4161/mabs.29938.
11. Bodier-Montagutelli E.; Respaud R.; Perret G.; Baptista L.; Duquenne P.; Heuzé-Vourc'h N.; L., V. Protein stability during nebulization: mind the collection step! . *European Journal of Pharmaceutics and Biopharmaceutics* 2020, doi:https://doi.org/10.1016/j.ejpb.2020.04.006.
12. Braun, A.; Kwee, L.; Labow, M.A.; Alsenz, J. Protein aggregates seem to play a key role among the parameters influencing the antigenicity of interferon alpha (IFN-alpha) in normal and transgenic mice. *Pharmaceutical research* 1997, 14, 1472-1478, doi:10.1023/a:1012193326789.
13. Joubert, M.K.; Hokom, M.; Eakin, C.; Zhou, L.; Deshpande, M.; Baker, M.P.; Goletz, T.J.; Kerwin, B.A.; Chirmule, N.; Narhi, L.O.; et al. Highly aggregated antibody therapeutics can enhance the *in vitro* innate and late-stage T-cell immune responses. *The Journal of biological chemistry* 2012, 287, 25266-25279, doi:10.1074/jbc.M111.330902.
14. Uchino, T.; Miyazaki, Y.; Yamazaki, T.; Kagawa, Y. Immunogenicity of protein aggregates of a monoclonal antibody generated by forced shaking stress with siliconized and nonsiliconized syringes in BALB/c mice. *The Journal of pharmacy and pharmacology* 2017, 69, 1341-1351, doi:10.1111/jphp.12765.
15. Mahlangu, J.N.; Weldingh, K.N.; Lentz, S.R.; Kaicker, S.; Karim, F.A.; Matsushita, T.; Recht, M.; Tomczak, W.; Windyga, J.; Ehrenforth, S.; et al. Changes in the amino acid sequence of the recombinant human factor VIIa analog, vatreptacog alfa, are associated with clinical immunogenicity. *Journal of thrombosis and haemostasis : JTH* 2015, 13, 1989-1998, doi:10.1111/jth.13141.

- 689 16. Holland, M.C.; Wurthner, J.U.; Morley, P.J.; Birchler, M.A.; Lambert, J.; Albayaty, M.; Serone, A.P.; Wilson, R.; Chen, Y.; For-
690 rest, R.M.; et al. Autoantibodies to variable heavy (VH) chain Ig sequences in humans impact the safety and clinical pharma-
691 cology of a VH domain antibody antagonist of TNF-alpha receptor 1. *Journal of clinical immunology* 2013, 33, 1192-1203,
692 doi:10.1007/s10875-013-9915-0.
- 693 17. Ponce, R.; Abad, L.; Amaravadi, L.; Gelzleichter, T.; Gore, E.; Green, J.; Gupta, S.; Herzyk, D.; Hurst, C.; Ivens, I.A.; et al. Im-
694 munogenicity of biologically-derived therapeutics: assessment and interpretation of nonclinical safety studies. *Regulatory*
695 *toxicology and pharmacology : RTP* 2009, 54, 164-182, doi:10.1016/j.yrtph.2009.03.012.
- 696 18. Schellekens, H. Bioequivalence and the immunogenicity of biopharmaceuticals. *Nature reviews. Drug discovery* 2002, 1,
697 457-462, doi:10.1038/nrd818.
- 698 19. Li, J.; Yang, C.; Xia, Y.; Bertino, A.; Glaspy, J.; Roberts, M.; Kuter, D.J. Thrombocytopenia caused by the development of anti-
699 bodies to thrombopoietin. *Blood* 2001, 98, 3241-3248, doi:10.1182/blood.v98.12.3241.
- 700 20. Demeule, B.; Gurny, R.; Arvinte, T. Where disease pathogenesis meets protein formulation: renal deposition of immuno-
701 globulin aggregates. *European journal of pharmaceuticals and biopharmaceutics : official journal of Arbeitsgemeinschaft fur*
702 *Pharmazeutische Verfahrenstechnik e.V* 2006, 62, 121-130, doi:10.1016/j.ejpb.2005.08.008.
- 703 21. Kiese, S.; Pappengerger, A.; Friess, W.; Mahler, H.C. Shaken, not stirred: mechanical stress testing of an IgG1 antibody.
704 *Journal of pharmaceutical sciences* 2008, 97, 4347-4366, doi:10.1002/jps.21328.
- 705 22. Fathallah, A.M.; Bankert, R.B.; Balu-Iyer, S.V. Immunogenicity of subcutaneously administered therapeutic proteins--a mech-
706 anistic perspective. *The AAPS journal* 2013, 15, 897-900, doi:10.1208/s12248-013-9510-6.
- 707 23. Mahler, H.C.; Friess, W.; Grauschopf, U.; Kiese, S. Protein aggregation: pathways, induction factors and analysis. *Journal of*
708 *pharmaceutical sciences* 2009, 98, 2909-2934, doi:10.1002/jps.21566.
- 709 24. Lamichhane, A.; Azegamia, T.; Kiyono, H. The mucosal immune system for vaccine development. *Vaccine* 2014, 32,
710 6711-6723, doi:10.1016/j.vaccine.2014.08.089.
- 711 25. Frank, D.W.; Vallis, A.; Wiener-Kronish, J.P.; Roy-Burman, A.; Spack, E.G.; Mullaney, B.P.; Megdoud, M.; Marks, J.D.; Fritz, R.;
712 Sawa, T. Generation and characterization of a protective monoclonal antibody to *Pseudomonas aeruginosa* PcrV. *The Journal*
713 *of infectious diseases* 2002, 186, 64-73, doi:10.1086/341069.
- 714 26. Lenz, A.G.; Stoeger, T.; Cei, D.; Schmidmeir, M.; Semren, N.; Burgstaller, G.; Lentner, B.; Eickelberg, O.; Meiners, S.; Schmid, O.
715 Efficient bioactive delivery of aerosolized drugs to human pulmonary epithelial cells cultured in air-liquid interface conditions.
716 *American journal of respiratory cell and molecular biology* 2014, 51, 526-535, doi:10.1165/rcmb.2013-0479OC.
- 717 27. Spadaro, M.; Montone, M.; Cavallo, F. Generation and Maturation of Human Monocyte-derived DCs *Bio-protocol* 2014, 4,
718 doi:10.21769/BioProtoc.1194.
- 719 28. Arganda-Carreras, I.; Kaynig, V.; Rueden, C.; Eliceiri, K.W.; Schindelin, J.; Cardona, A.; Sebastian Seung, H. Trainable Weka
720 Segmentation: a machine learning tool for microscopy pixel classification. *Bioinformatics* 2017, 33, 2424-2426,
721 doi:10.1093/bioinformatics/btx180.
- 722 29. Zolls, S.; Tantilpolphan, R.; Wigggenhorn, M.; Winter, G.; Jiskoot, W.; Friess, W.; Hawe, A. Particles in therapeutic protein for-
723 mulations, Part 1: overview of analytical methods. *Journal of pharmaceutical sciences* 2012, 101, 914-935, doi:10.1002/jps.23001.
- 724 30. EMA. Guideline on Immunogenicity assessment of therapeutic proteins. 2017.
- 725 31. FDA. Immunogenicity Assessment for Therapeutic Protein Products - Guidance for Industry. 2014.
- 726 32. Galluzzi, L.; Bravo-San Pedro, J.M.; Kepp, O.; Kroemer, G. Regulated cell death and adaptive stress responses. *Cellular and*
727 *molecular life sciences : CMLS* 2016, 73, 2405-2410, doi:10.1007/s00018-016-2209-y.
- 728 33. Galluzzi, L.; Bravo-San Pedro, J.M.; Vitale, I.; Aaronson, S.A.; Abrams, J.M.; Adam, D.; Alnemri, E.S.; Altucci, L.; Andrews, D.;
729 Annicchiarico-Petruzzelli, M.; et al. Essential versus accessory aspects of cell death: recommendations of the NCCD 2015. *Cell*
730 *death and differentiation* 2015, 22, 58-73, doi:10.1038/cdd.2014.137.
- 731 34. Vermes, I.; Haanen, C.; Steffens-Nakken, H.; Reutelingsperger, C. A novel assay for apoptosis. Flow cytometric detection of
732 phosphatidylserine expression on early apoptotic cells using fluorescein labelled Annexin V. *Journal of immunological*
733 *methods* 1995, 184, 39-51, doi:10.1016/0022-1759(95)00072-i.
- 734 35. Moussa, E.M.; Panchal, J.P.; Moorthy, B.S.; Blum, J.S.; Joubert, M.K.; Narhi, L.O.; Topp, E.M. Immunogenicity of Therapeutic
735 Protein Aggregates. *Journal of pharmaceutical sciences* 2016, 105, 417-430, doi:10.1016/j.xphs.2015.11.002.
- 736 36. Ratanji, K.D.; Derrick, J.P.; Dearman, R.J.; Kimber, I. Immunogenicity of therapeutic proteins: influence of aggregation. *Journal*
737 *of immunotoxicology* 2014, 11, 99-109, doi:10.3109/1547691X.2013.821564.
- 738 37. Ross, C.; Clemmesen, K.M.; Svenson, M.; Sorensen, P.S.; Koch-Henriksen, N.; Skovgaard, G.L.; Bendtzen, K. Immunogenicity
739 of interferon-beta in multiple sclerosis patients: influence of preparation, dosage, dose frequency, and route of administration.
740 *Danish Multiple Sclerosis Study Group. Annals of neurology* 2000, 48, 706-712.
- 741 38. Hermeling, S.; Schellekens, H.; Crommelin, D.J.; Jiskoot, W. Micelle-associated protein in epoetin formulations: aA risk factor
742 for immunogenicity? *Pharmaceutical research* 2003, 20, 1903-1907, doi:10.1023/b:pham.0000008034.61317.02.
- 743 39. Cromwell, M.E.; Hilario, E.; Jacobson, F. Protein aggregation and bioprocessing. *The AAPS journal* 2006, 8, E572-579,
744 doi:10.1208/aapsj080366.
- 745 40. Joubert, M.K.; Luo, Q.; Nashed-Samuel, Y.; Wypych, J.; Narhi, L.O. Classification and characterization of therapeutic antibody
746 aggregates. *The Journal of biological chemistry* 2011, 286, 25118-25133, doi:10.1074/jbc.M110.160457.

- 747 41. Wang, W. Protein aggregation and its inhibition in biopharmaceutics. *International journal of pharmaceutics* 2005, 289, 1-30,
748 doi:10.1016/j.ijpharm.2004.11.014.
- 749 42. Lightwood, D.; O'Dowd, V.; Carrington, B.; Veverka, V.; Carr, M.D.; Tservistas, M.; Henry, A.J.; Smith, B.; Tyson, K.; Lamour,
750 S.; et al. The discovery, engineering and characterisation of a highly potent anti-human IL-13 fab fragment designed for ad-
751 ministration by inhalation. *Journal of molecular biology* 2013, 425, 577-593, doi:10.1016/j.jmb.2012.11.036.
- 752 43. Maillet, A.; Congy-Jolivet, N.; Le Guellec, S.; Vecellio, L.; Hamard, S.; Courty, Y.; Courtois, A.; Gauthier, F.; Diot, P.; Thibault,
753 G.; et al. Aerodynamical, immunological and pharmacological properties of the anticancer antibody cetuximab following
754 nebulization. *Pharmaceutical research* 2008, 25, 1318-1326, doi:10.1007/s11095-007-9481-3.
- 755 44. Kraus, T.; Winter, G.; Engert, J. Test models for the evaluation of immunogenicity of protein aggregates. *International journal*
756 *of pharmaceutics* 2019, 559, 192-200, doi:10.1016/j.ijpharm.2019.01.015.
- 757 45. Carpenter, J.F.; Randolph, T.W.; Jiskoot, W.; Crommelin, D.J.; Middaugh, C.R.; Winter, G.; Fan, Y.X.; Kirshner, S.; Verthelyi, D.;
758 Kozlowski, S.; et al. Overlooking subvisible particles in therapeutic protein products: gaps that may compromise product
759 quality. *Journal of pharmaceutical sciences* 2009, 98, 1201-1205, doi:10.1002/jps.21530.
- 760 46. Telikeyalli, S.; Kumru, O.S.; Kim, J.H.; Joshi, S.B.; O'Berry, K.B.; Blake-Haskins, A.W.; Perkins, M.D.; Middaugh, C.R.; Volkin,
761 D.B. Characterization of the physical stability of a lyophilized IgG1 mAb after accelerated shipping-like stress. *Journal of*
762 *pharmaceutical sciences* 2015, 104, 495-507, doi:10.1002/jps.24242.
- 763 47. Xiang, S.D.; Scholzen, A.; Minigo, G.; David, C.; Apostolopoulos, V.; Mottram, P.L.; Plebanski, M. Pathogen recognition and
764 development of particulate vaccines: does size matter? *Methods* 2006, 40, 1-9, doi:10.1016/j.ymeth.2006.05.016.
- 765 48. Hertel, S.; Friess, W.; Winter, G. Comparison of Aerosol Collection Methods for Liquid Protein Formulations; 2011.
- 766 49. Brandenberger, C.; Muhlfeld, C.; Ali, Z.; Lenz, A.G.; Schmid, O.; Parak, W.J.; Gehr, P.; Rothen-Rutishauser, B. Quantitative
767 evaluation of cellular uptake and trafficking of plain and polyethylene glycol-coated gold nanoparticles. *Small* 2010, 6,
768 1669-1678, doi:10.1002/smll.201000528.
- 769 50. Brandenberger, C.; Rothen-Rutishauser, B.; Muhlfeld, C.; Schmid, O.; Ferron, G.A.; Maier, K.L.; Gehr, P.; Lenz, A.G. Effects and
770 uptake of gold nanoparticles deposited at the air-liquid interface of a human epithelial airway model. *Toxicology and applied*
771 *pharmacology* 2010, 242, 56-65, doi:10.1016/j.taap.2009.09.014.
- 772 51. Rohm, M.; Carle, S.; Maigler, F.; Flamm, J.; Kramer, V.; Mavoungou, C.; Schmid, O.; Schindowski, K. A comprehensive
773 screening platform for aerosolizable protein formulations for intranasal and pulmonary drug delivery. *International journal of*
774 *pharmaceutics* 2017, 532, 537-546, doi:10.1016/j.ijpharm.2017.09.027.
- 775 52. Shomali, M.; Freitag, A.; Engert, J.; Siedler, M.; Kaymakcalan, Z.; Winter, G.; Carpenter, J.F.; Randolph, T.W. Antibody re-
776 sponses in mice to particles formed from adsorption of a murine monoclonal antibody onto glass microparticles. *Journal of*
777 *pharmaceutical sciences* 2014, 103, 78-89, doi:10.1002/jps.23772.
- 778 53. Freitag, A.J.; Shomali, M.; Michalakis, S.; Biel, M.; Siedler, M.; Kaymakcalan, Z.; Carpenter, J.F.; Randolph, T.W.; Winter, G.;
779 Engert, J. Investigation of the immunogenicity of different types of aggregates of a murine monoclonal antibody in mice.
780 *Pharmaceutical research* 2015, 32, 430-444, doi:10.1007/s11095-014-1472-6.
- 781 54. Lim, J.; Yue, Z. Neuronal aggregates: formation, clearance, and spreading. *Developmental cell* 2015, 32, 491-501,
782 doi:10.1016/j.devcel.2015.02.002.
- 783 55. Bucciantini, M.; Calloni, G.; Chiti, F.; Formigli, L.; Nosi, D.; Dobson, C.M.; Stefani, M. Prefibrillar amyloid protein aggregates
784 share common features of cytotoxicity. *The Journal of biological chemistry* 2004, 279, 31374-31382, doi:10.1074/jbc.M400348200.
- 785 56. Dingman, R.; Balu-Iyer, S.V. Immunogenicity of Protein Pharmaceuticals. *Journal of pharmaceutical sciences* 2019, 108,
786 1637-1654, doi:10.1016/j.xphs.2018.12.014.